Supplementary Materials

Human Microsaccade-Related Visual Brain Responses

Olaf Dimigen, Matteo Valsecchi, Werner Sommer, & Reinhold Kliegl

Figure S1

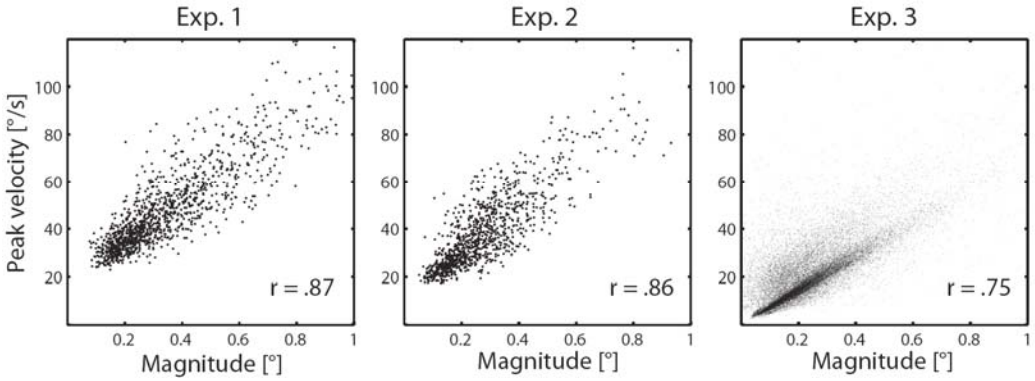

Magnitude-velocity relationship of microsaccades in the three experiments. The linear relationship ('main sequence', Zuber et al., 1965) is indicative of the fact that the events detected by the algorithm were microsaccades.

Figure S2

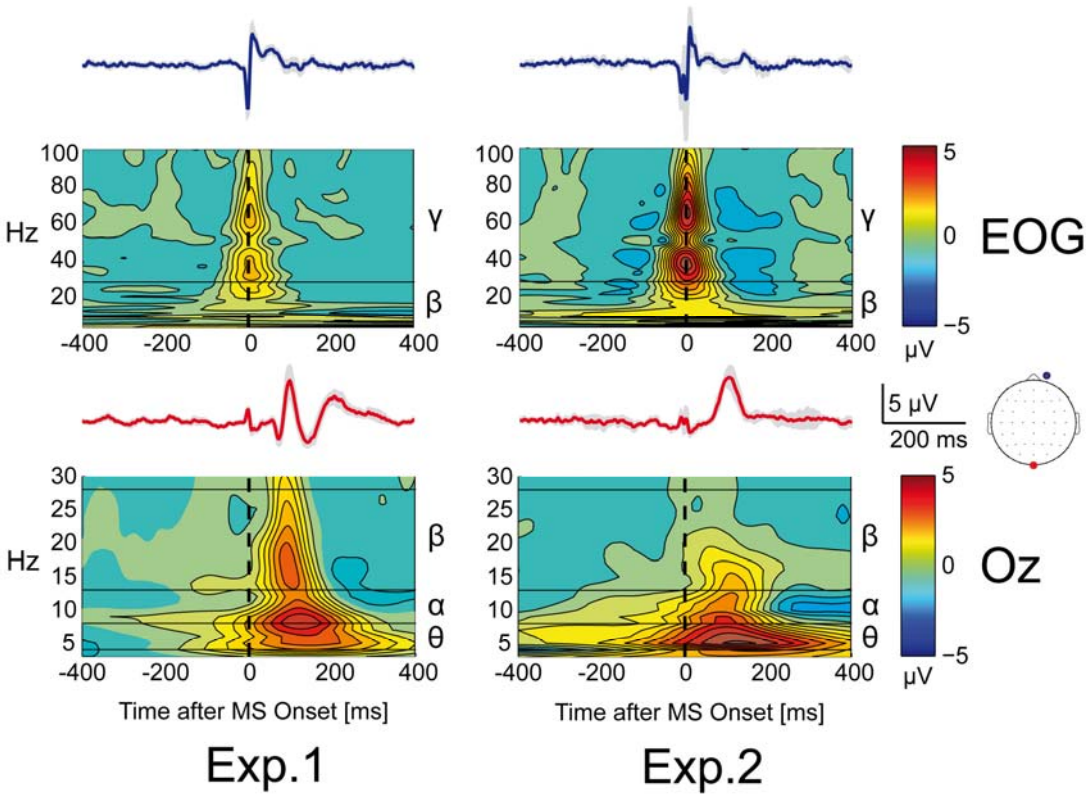

Grand mean ERP and time-frequency plots for microsaccade-related potentials in experiments 1 and 2. *Upper panels:* Data for the right infraorbital EOG electrode, where the microsaccadic spike potential (SP, visible in the averaged ERP trace) was largest. The wavelet transform was applied to individual microsaccade-locked segments and then averaged (see *Materials and Methods for Figure S2*). The transient SP translated to an increase in spectral power in the high beta and gamma band at movement onset. Because microsaccades occur with temporal jitter in each trial, microsaccadic SPs can mimic an increase in the power of "induced" (non-phase-locked) gamma band oscillations (Yuval-Greenberg et al., 2008). Horizontal lines indicate frequency band limits. The power reduction at 50 Hz is due to the notch filter. *Lower panels:* Data at occipital electrode Oz. The waveform of the microsaccadic lambda response (MLR) translated to a broadband increase in spectral power with a maximum in the theta and lower alpha band about 100 ms after microsaccade onset.

Methods for Figure S2

Time-frequency analyses were performed by convolving each microsaccade-locked EEG segment with a family of complex Morlet's wavelets (Tallon-Baudry and Bertrand, 1999) using the wavelet function in the BrainVision Analyzer Software (v1.05, Brain Products GmbH, Germany). Wavelet calculation was performed on a set of microsaccade-locked segments that was longer (from – 2000 to 1500 ms) and notch-filtered with a 50 ± 2 Hz (48 dB) band rejection filter to eliminate a line noise artifact emitted by the near-by eye tracking hardware. Wavelets were applied to center frequencies from 3 to 100 Hz in steps of 1 Hz. The constant ratio $m = F_0/\sigma_f$ (where F_0 is the wavelet's center frequency and σ_f its SD in the frequency domain) was set to $m = 12$ for the analysis of high frequencies (upper panels) and $m = 6$ for low frequencies (3-30 Hz, lower panels). Single-trial scalograms were baseline-corrected by subtracting at each frequency the mean activity from -1500 to - 1000 ms before microsaccade onset. An early baseline was chosen to avoid temporal smearing of microsaccade-related activity into the baseline at low frequencies (Herrmann et al., 2005). Time-frequency data was first averaged within each subject, and then collapsed across subjects.

Figure S3

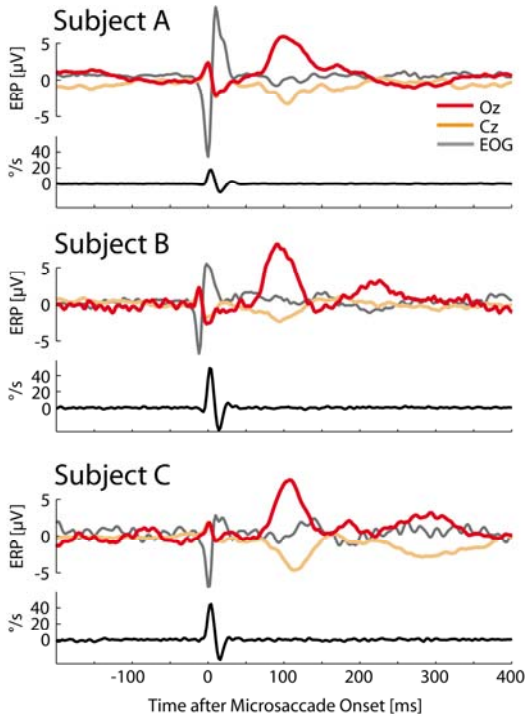

Single subject averages for Exp. 2 (sustained face fixation). Microsaccade-related potentials are shown for Oz, Cz, and the right infraorbital EOG electrode. Lower traces show eye velocity; negative velocities represent movements against the predominant orientation of the microsaccade. In one of the subjects (subject B), the spike potential peaked already 10 ms before the detected movement onset in the eye track, causing a double spike in the grand-averaged data (shown in Fig. 3).

Figure S4

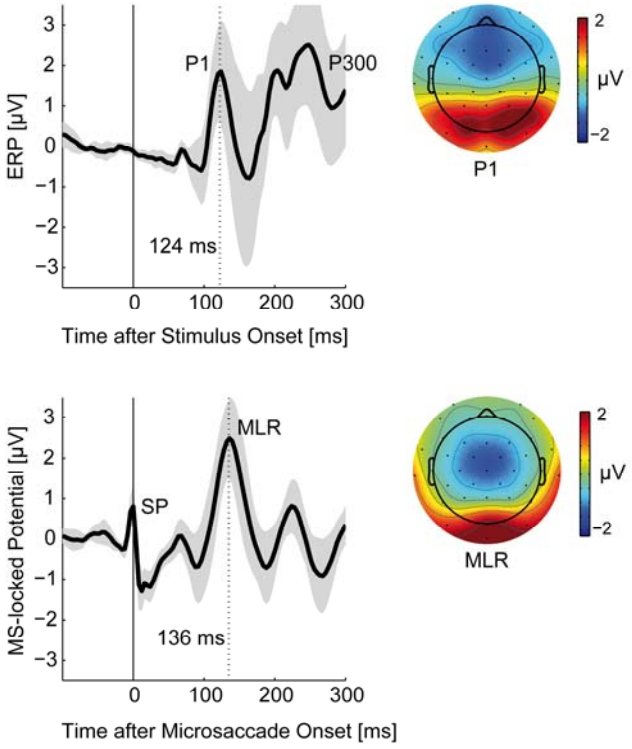

Comparison of stimulus-evoked and microsaccade-evoked potentials in the oddball experiment (Exp. 3). Data is shown for occipital electrode Oz. Shading indicates 95% between-subject confidence intervals. *Upper panel*: ERP time-locked to the onset of the red or green disc stimulus. The P1 component of the visual evoked potential (VEP) peaked after 124 ms, followed by the endogenous P300 component, which was also visible at occipital sites. *Lower panel*: ERP time-locked to the onset of microsaccades, detected during the trials of the oddball task. SP = spike potential. The microsaccadic lambda response (MLR) peaked after 136 ms. Scalp topographies are shown at the respective peak latencies of the P1 and MLR. Electrodes below the horizontal meridian are plotted outside the head perimeter. Note that the MLR, which frequently overlapped the stimulus-locked EEG epochs, was of similar amplitude as the VEP evoked by stimulus onset.

Figure S5 (follow-up experiment)

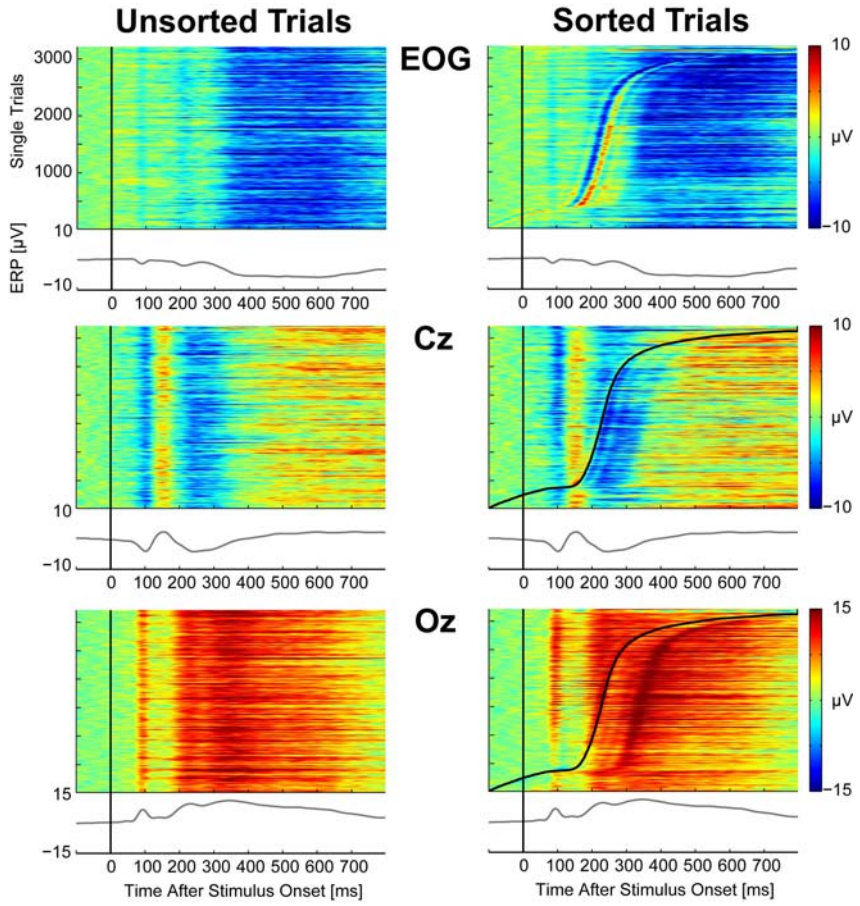

Impact of small saccades on stimulus-locked ERPs in a face classification experiment with large pictorial stimuli, long stimulus duration, standard fixation instructions, and no embedded fixation point (see *Materials and Methods for Fig. S5*). Single-trial EEG segments from twelve subjects are shown. Time 0 indicates the onset of the face stimulus that required a manual choice reaction. Bottom panels of each plot show the stimulus-locked ERP (grey line) that is obtained by averaging at each time point ("vertically") across all trials. *Left column*: The impact of saccades is not evident when segments are plotted in random order. *Right column*: Same data, after sorting by the latency of the first microsaccade or saccade (black line) detected in each trial. Despite an EOG-based artifact rejection, at least one saccade was observed in 95% of the segments, with a median magnitude of 1.58° (±0.41). The muscle SP is visible in the mean signal from the left and right horizontal EOG electrode ("EOG"). Plots for electrodes Cz and Oz show how saccadic lambda responses alter the ERP morphology. For example, the negative ERP deflection at Cz between 200-300 ms can be partially attributed to microsaccade-evoked potentials. Similarly, at electrode Oz, the late positive complex (LPC) is increased by overlapping lambda responses.

Materials and Methods for Figure S5 (follow-up experiment)

Subjects. Twelve healthy students (8 female, 19-35 years) participated after providing written informed consent. Subjects were different from those tested in Exp. 1-3 and naïve as to the purpose of the experiment.

Stimuli. Color portraits (7.5° × 8.5°) of 40 male or female persons (see Fig. 3a) were used. The face of each person was shown with three emotional expressions (anger, happiness, or neutral expression), leading to a set of 120 stimuli. Faces were presented on a 14 cd/m^2 gray background at a monitor refresh rate of 120 Hz and a resolution of 1024x768 pixels. In contrast to Exp. 2, face stimuli did not include a fixation point. Presentation hardware was identical to Exp. 1 and 2.

Procedure. Subjects performed a speeded manual classification of the face's emotional expression. Responses were given with three keys, operated with the index, middle, and ring finger of the right hand. In each of four experimental blocks, all 120 stimuli were presented in random order. At the beginning of a trial, a 0.26° white fixation cross was presented on a gray screen for 1000 ms. It was immediately followed by the face, which remained on screen for 1350 ms. Subjects received standard written instructions to minimize blinks and eye movements while the stimulus was visible.

FEM and EEG recording. FEM were recorded binocularly at a rate of 500 Hz using the same eye tracker as in Exp. 1 and 2. Microsaccades and saccades were detected with the algorithm and parameters described for Exp. 1, with the additional constraint of binocularity (i.e. high-velocity movements were only classified as (micro)saccades if they occurred with temporal overlap in both eyes). The EEG recording setup was identical to Exp. 3. Offline, EEG channels were filtered with a bandpass from 0.1 to 30 Hz and re-referenced against the average of all channels.

Data analyses. EEG segments of 900 ms (-100 to 800 ms) were cut around each stimulus onset and baseline-corrected with a 100 ms pre-stimulus baseline. We rejected all segments with eye blinks or large saccades (> 3°) in the concurrent eye track. Additionally, an EOG-based rejection threshold was applied: All segments were rejected in which the horizontal or vertical bipolar EOG exceeded ±75 μV. The remaining segments (56%) were then sorted according to the latency of the first microsaccade or saccade detected in the eye tracking data of the respective trial. For visualization, trials were smoothed with a moving average across 20 adjacent trials after sorting.

References for Supplement

Herrmann CS, Grigutsch M, Busch NA (2005) EEG oscillations and wavelet analysis. In: Event-related potentials: a methods handbook (Handy T, ed.), p 229-259. Cambridge: MIT Press.

Tallon-Baudry C, Bertrand O (1999) Oscillatory gamma activity in humans and its role in object representation. Trends Cogn Sci 3:151-162.

Yuval-Greenberg S, Tomer O, Keren AS, Nelken I, Deouell LY (2008) Transient induced gamma-band response in EEG as a manifestation of miniature saccades. Neuron 58:429-441.

Zuber BL, Stark L, Cook G (1965) Microsaccades and the velocity-amplitude relationship for saccadic eye movements. Science 150:1459-1460.